Journal of ELECTRICAL ENGINEERING, VOL 73(2022), NO1, 43–49

sciendo

PAPERS

Fabrication of PDMS chips by laser engraving for protein enrichments

Linlin Sun[1,3], Ao Ding[1], Yangbo Chen[2], Xue Yang[1], Zhifu Yin[1,2,*], Yuqiang Fang[1,*]

PDMS (Polydimethylsiloxane) chips are increasingly important for the application of fluorescence measurements due to their auto-fluorescence free, excellent transparency, and biocompatibility. However, the design of PDMS microfluidic chips requires to fabricate plenty of molds for structure optimization, resulting in high cost. In the present, PDMS chips with nafion membrane were fabricated by simple and low-cost method for bull serum albumin (BSA) enrichment. To optimize the laser cutting and bonding parameters, simulation models were established using Bilinear Kinematic and Mooney-Rivlin models, respectively. The influence of laser power and cutting speed on the width and depth of the micro-channels was investigated. And the effect of bonding pressure on the deformation of PDMS micro-channel and stress distribution near the micro-channels was also analyzed. The leakage test and BSA enrichment demonstrated the practicability and feasibility of the present fabrication method in this work.

K e y w o r d s: microfluidic chip, laser cutting, protein enrichment, numerical simulation

1 Introduction

Microfluidic chips has both their width and depth in the micro-scale, which in the same order of biological substances such as cells, blood vessels, and nerves [1]. They have great potentials for the analysis, control and manipulation of those biological substances at micro-scale. Microfluidic chips are becoming increasingly important for biological, medical and chemical applications due to the special phenomena only occur in micro-channels [2]. For example, heat could transfer extremely fast, in several second, between channels due to the small size of the chip[3]. Capillary force can be improved due to the high surface-to-volume ratio of the micro-channels [4]. Labeled proteins and ions could enriched near the nafion film in the micro-channel resulting from the electric double layer near the film [5, 6]. At present, those minimized chips have already be used in a wide range of applications.

Microfluidic chips are always single-use to avoid any measuring interference caused by the residual sample in the channel. Thus the cost of the chips is a critical issue for their commercialization. Polymer and paper microfluidic chips have been developed to replace traditional silicon, glass, and quartz chips [7, 8]. Paper chips can hardly control the flow speed of the fluid and the evaporation of the fluid cannot be prevented [9]. Therefore, polymer chips are still be widely used, such as Polymethyl Methacrylate (PMMA), Polyethylene Terephthalate (PET), Polycarbonate (PC), and Polydimethylsiloxane (PDMS) chips [10]. The micro-channels could be easily patterned by traditional low cost methods (hot embossing, injection molding or casting methods). The cost could be further decreased when the chips are fabricated in volume production. Above polymer, except for PDMS, suffer from high auto-fluorescence when excited by ultraviolet light. Auto-fluorescence is the natural fluorescence of the polymer excited by ultraviolet light without adding any fluorescent material. Usually the intensity of the polymer is larger than that emitted by the proteins, making the useful fluorescence invisible [11]. In terms of auto-fluorescence, PDMS is an ideal material for fluorescence measurements. Now, it has been one of the most commonly used material for microfluidic chips due to its biocompatibility, auto-fluorescent free, and excellent flexibility [12].

PDMS micro-channels [13, 14] or even nano-channels [15, 16] can be fabricated by PDMS casting. However, to fabricate PDMS chips by casting method, convex hard-molds should be fabricated before PDMS casting step. It is always costly to pattern hard-molds, such as silicon, glass, or SU-8 molds. In addition, the shape and size of the micro-channels should be optimized to obtain a best performance for a specific application. Thus, many hard-molds should be fabricated at design stage of the microfluidic chip. This brings about the consequent time-consuming and cost issues. CO2 laser is an affordable equipment for most of researchers. Micro-channels could be easily patterned in to PDMS slab with width and depth ranging from tens to hundreds of micro-meters [17-19]. Since it could produce desired complex patterns in

[1] School of Mechanical and Aerospace Engineering, Jilin University, Changchun 130025, China, [2] The State Key Laboratory of Alternate Electrical Power System with Renewable Energy Sources, North China Electric Power University, Beijing, 100096, China, [3] State Key Laboratory of Luminescent Materials and Devices, South China University of Technology, Guangzhou 510640, China, * Corresponding authors: yinzf@jlu.edu.cn; yuqiangfang@jlu.edu.cn

https://doi.org/10.2478/jee-2022-0006, Print (till 2015) ISSN 1335-3632, On-line ISSN 1339-309X

most of polymers without using any mold, it has already been employed in a wide range of industrial and scientific researches. It is know that three main factors could affect the size of patterned micro-channels. They are laser spot size, laser power, and cutting speed [20, 21]. The size of the micro-channels is associated with lager spot size and laser power, while associated with lower cutting speed. Some scholars also took cutting passes into consideration [22]. The size of the micro-channels will be enlarged by more cutting passes. Thus, by optimizing the cutting parameters PDMS micro-channels could be fabricated with desired width and depth. CO2 laser cutting becomes an ideal approach to produce micro-channels in PDMS slab.

In the present paper, laser cutting was employed to fabricate low-cost PDMS chips. The temperature distribution in PDMS slabs during laser cutting was investigated. To fabricate desired micro-channel, the influence of laser power and cutting speed on the width and depth of the micro-channels was investigated. To fully bond the micro-channel, the influence of bonding pressure on the deformation of PDMS micro-channel and stress distribution in the micro-channels was also analyzed by numerical simulation. The chip was finally used for albumin enrichment to identify the fabrication quality.

2 Experimental details

In this work, a commercial PDMS (Sylgard 184, Dow Corning, Michigan, USA) was used to produce PDMS slab. PDMS slabs were fabricated by PDMS casting on a glass slide [15]:

(1) PDMS pre-polymer and curing agent with weight ratio 10:1 were mixed thoroughly by stirring with a glass rod in a disposable plastic cup.

(2) The mixture was degassed in a vacuum oven at 2 Pa for 20 min to eliminate the trapped air bubble in the mixture.

(3) The cleaned glass slab was fenced by scotch tape forming a container.

(4) The degassed mixture was poured onto glass slab and degassed again in the vacuum oven at 2 Pa for 30 min.

(5) The glass container with the mixture was heated in the vacuum oven at 90 C for 1h to fully cure PDMS.

(6) The cured PDMS was peeled from the glass and then cut by a scalpel to form flat PDMS slabs.

The fabrication procedures of PDMS microfluidic chip for protein enrichment is shown as in Fig. 1. The CO_2 laser machine (3020 type, Yongsheng laser Co., Ltd, Shandong, China) was used to pattern PDMS slabs. As shown in Fig. 1(a), the desired linear micro-channel was fabricated in both upper and lower PDMS slabs by laser cutting. Four reservoirs were punched in upper PDMS slab by hole puncher, Fig. 1(b). After ultrasonic cleaning, and drying, PDMS slabs and nafion membrane were oxygen plasma treated for 10 s. To fully bond PDMS slabs and nafion together after alignment, Fig. 1(d), a necessary bonding pressure was applied on them by clamps. After heated at 200 °Cfor 1 min, PDMS microfluidic chip was finally fabricated.

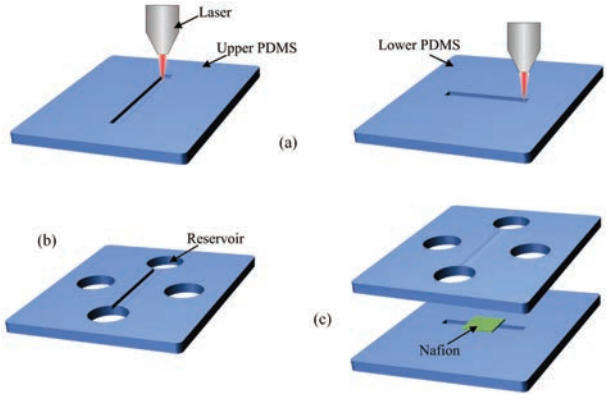

Fig. 1. Fabrication of PDMS microfluidic chip: (a) – laser cutting in both upper and lower PDMS, (b) – reservoirs punching on upper PDMS, (c) – bonding of PDMS slabs and nafion membrane, and (d) – schematic profile of fabricated chip

3 Results and discussion

3.1 Temperature field distribution during laser cutting

In the paper, numerical simulation was adopted to analyze the temperature distribution in PDMS slab during laser cutting. A 3D geometric model was established with the same size of that used for experiment. PDMS slab was considered to be a bilinear kinematic model. The elements near the laser were refined to improve the simulation accuracy. The distribution of laser beam was considered to be an ideal Gauss distribution. The intensity of the laser beam is given by the following equation, [23]

$$I(x,y,z) = \frac{2P}{\pi R(z)^2} \exp\Big(\frac{-2r^2}{R(z)^2}\Big)\,, \tag{1}$$

where, P is the laser power, $R(z)$ is the beam radius at any cutting depth z into the PDMS slab, and r is the distance from the computational element to the center of laser beam, which is,

$$r = \sqrt{(x-x_0)^2 + (y-y_0)^2}\,. \tag{2}$$

The laser beam radius along the z axis can be calculated as

$$R(z) = R_0\sqrt{1+\frac{z}{R_\mathrm{a}}}\,, \tag{3}$$

where, R_0 is the radius of the focused laser beam and R_a is the Rayleigh length.

Figure 2 shows the temperature distribution in PDMS slab during laser cutting. It can be seen that the highest temperature lies in the center of the laser beam, which could be several thousand degree. The area of the highest temperature (red zone) is nearly equal to the spot size of

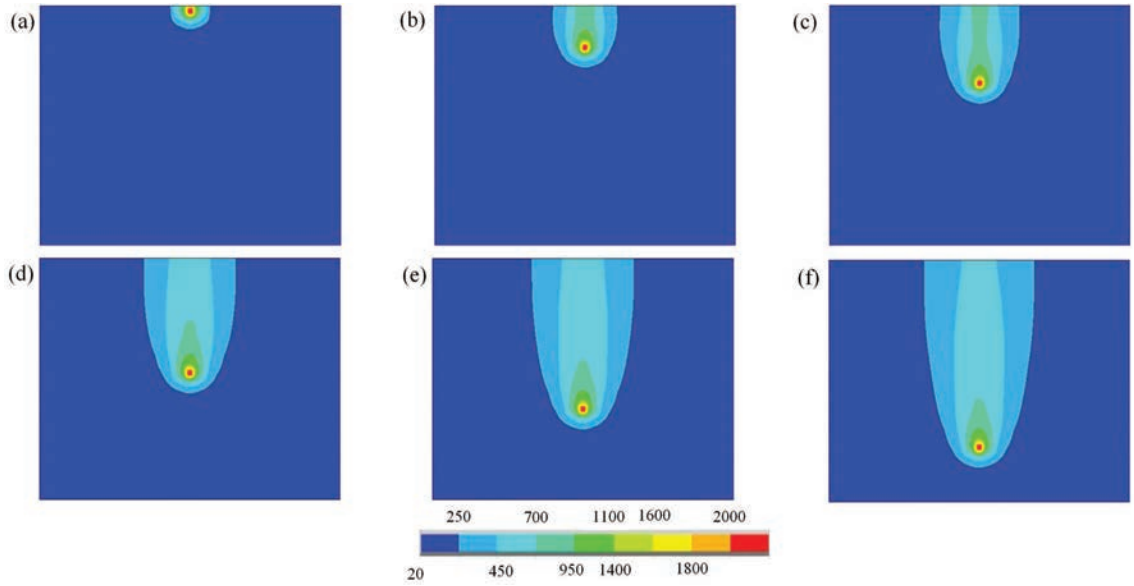

Fig. 2. The temperature distribution during laser cutting

the laser beam. This indicates that the width of the fabricated micro-channel greatly affected by the spot size. However, the width could be much larger than the spot size. This is because the melt temperature of most polymer is at several hundred temperature. Whereas, the temperature near the spot area could be two thousand degree. The width of the micro-channel will be much larger than the spot size. The moving speed of the laser beam also could affect the channel size. The effective cutting time is associated with laser moving speed. At low cutting speed, more PDMS will melt and be gasified, resulting in larger channel width and depth. The power of the laser beam can also influence the size of the channel. From (1), one can see that intensity of the laser beam is proportional to the laser power. As laser intensity increases, the temperature near the laser spot improves. The width and depth of the fabricated micro-channel will increase as well.

3.2 The influence of cutting parameters on the size of the micro-channels

According to (1) and the numerical simulation results, the size of the micro-channels could be influenced by three main laser parameters. Larger width and depth are associated with higher laser power, larger spot size and lower cutting speed. However, quantitative research should be performed. Thus the influence of cutting parameters on the size of the micro-channels was investigated by experiments. Since the spot size of the laser beam is fixed for our equipment, we only considered laser power and cutting speed in this study. In this study we found that at laser power higher than 20 W $\rightarrow$ PDMS could easily be cut off and under cutting speed larger than 35 mm/s the uniformity of the micro-channel could hardly be guaranteed. According to this, laser powers ranging from 10 to 20 W were selected, while cutting speeds ranging from 10 to 35 mm/s were chosen.

Figure 3(a) shows the effect of laser power on the width and depth of the micro-channels. The average width and depth were calculated by three measurements using three samples. Higher width and depth correlate to larger power. However, channel width and depth are not directly proportional to laser power. When laser power increases from $10\,\text{to}\,16\,W$, the width increases from 74 to $230\,\mu$m , and the depth increases from 17 to $335\,\mu$m. When laser power increases from 16 to 20 W, the width only increases from $230\,\text{to}\,243\,\mu$m, and the depth only increases from $335\,\text{to}\,398\,\mu$m. In other words, both channel width and depth increase significantly (10 to 16 W) firstly and then slightly (16 to 20 W). According to the data in Fig. 3(a), one could also see that the minimal width and depth are 74 and $17\,\mu$m, respectively. The maximal ones are $243\,\text{and}\,398\,\mu$m, respectively. The channel width increases by 169 μm , while depth increases by 381 μm . Therefore, laser power affect channel width more significantly than channel depth.

Figure 3(b) shows the effect of cutting speed on the width and depth of the micro-channels. When cutting speed increases from 10 to 35 mm/s, the width decrease from 192 to 127 m, and the depth decrease from 210 to 90 μm . For both channel width and depth, they nearly follow a simple linear regression based on cutting speed. A significant regression equations were found with a coefficient of determination, $R^2 = 0.97$ and 0.99 for channel width and depth. The channel width (W_c) could be predicted from cutting speed by the formula: $W_c = 218.07 - 2.46\,V_c$, where V_c is the cutting speed. The channel depth (D_c) could be predicted by the following formula $D_c = 267.14 - 5.07\,V_c$.

3.3 Sealing of the open micro-channel

After laser cutting, the open channel should be bonded to form a sealed micro-channel. In the present work, the open PDMS micro-channel was bonded with another

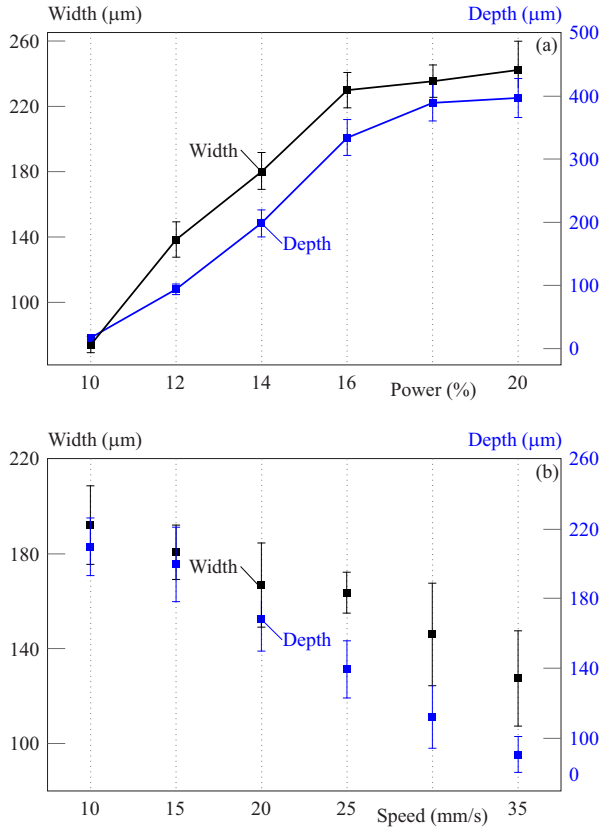

Fig. 3. The influence of a) laser power and b) cutting speed on the width and depth of the micro-channels

PDMS slab. Two crossed micro-channels were sealed as shown in Fig. 1c. In the center of the chip, there is a nafion membrane with a thickness of 25 μm . This will affect the bonding of PDMS slabs. It is hard to fully bond PDMS slabs together by traditional PDMS bond method (without applying any bonding pressure) [14]. To fully bond the chip, an additional pressure was applied by the clamps. However, the bonding pressure should be optimized. At high pressure, the chip could be fully sealed, but the micro-channel will be seriously deformed. Under low pressure, the micro-channel could be intact, whereas the chip will be partially bonded. The bonding pressure was optimized by numerical simulation. The influence of bonding pressure on the deformation of the micro-channels and stress distribution near the micro-channels was investigated. During numerical simulation, Mooney-Rivlin model was used to present PDMS slabs, since the cured PDMS was hyper-elastic. The Mooney-Rivlin model can be expressed as following [24],

$$W = C_{10}(I_1 - 3) + C_{01}(I_2 - 3), \tag{4}$$

where, W is the strain energy, C_{10}, C_{01} are physical constants characterizing the PDMS, and I_1, I_2 are strain invariants.

The physical constants C_{10}, C_{01} can be evaluated by Young's modulus of PDMS [25],

$$C_01 = 0.25 \times C_{10}, \tag{5}$$

$$6 \times (C_{10} + C_{01}) \approx E, \tag{6}$$

where, E is the Young's modulus of the PDMS. It could be founded in the articles [26, 27].

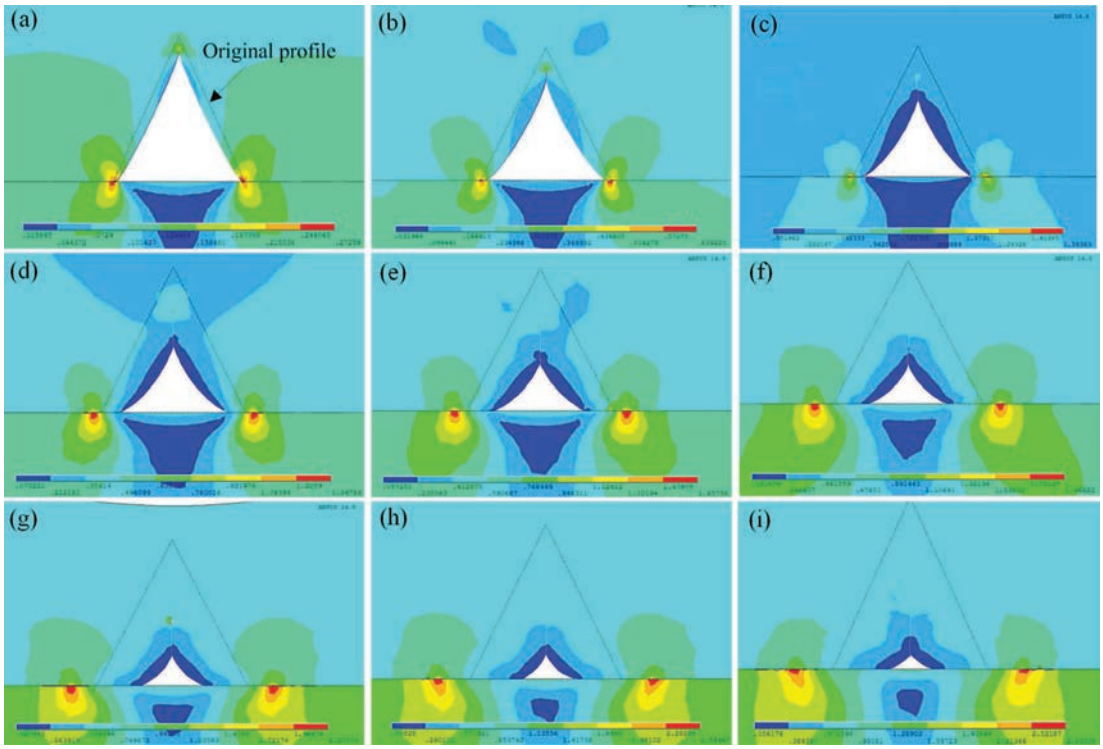

Fig. 4. The influence of bonding pressure on the deformation of the micro-channels

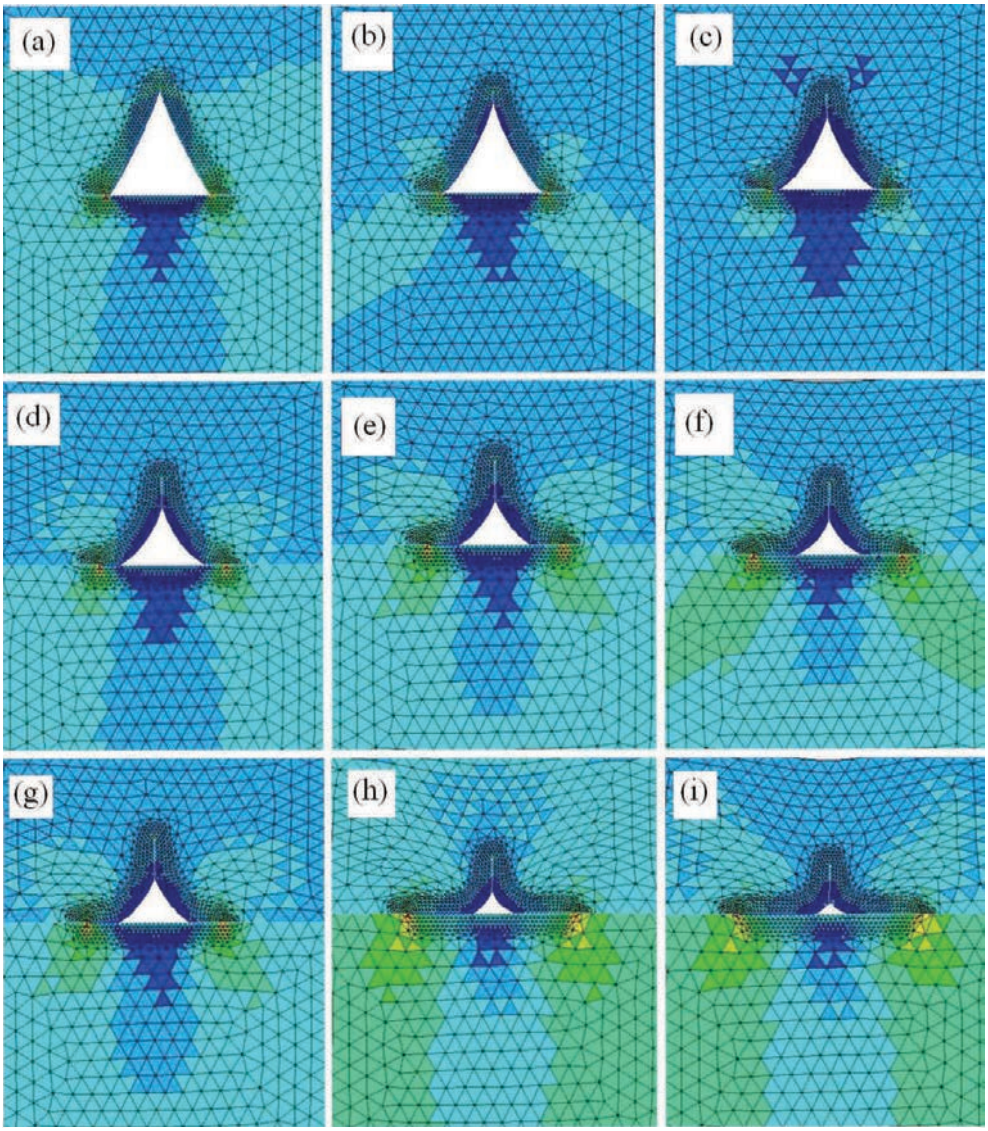

Fig. 5. The influence of bonding pressure on the stress distribution near the micro-channels

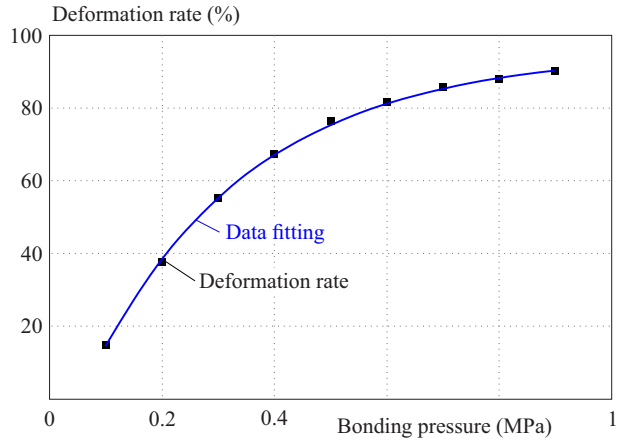

Fig. 6. The deformation rate of PDMS micro-channel after bonding under different pressure

PDMS slabs were oxygen plasma treated, hydroxyls (-OH) were generated on PDMS surface. During the bonding process, the hydroxyl (OH) on upper PDMS slab react with the one on lower PDMS slab, and then a chemical bond (O) and H2O will generate. Connected by the chemical bond, the upper and lower PDMS slabs cannot be separated. In this study, the additional pressure was applied, the micro-channel will deform and the inner-wall of the channel will contact together. The hydroxyl will also lead to the irreversible bonding of inner-wall after contacting. To present this bonding process in numerical simulation, a no separation boundary condition was used (once contact, cannot be separated) on the interface between upper and lower PDMS slabs and the inner-walls of the micro-channel. To improve the simulation precision, elements near the interface between PDMS slabs and the inner-wall of the channel were refined.

Figure 4 shows the numerical simulation results for bonding of PDMS micro-channel. It shows the influence of bonding pressure on the deformation of the micro-channels. The bonding pressure ranged from 0.1 to 0.9 MPa. To calculate the deformation of the channel,

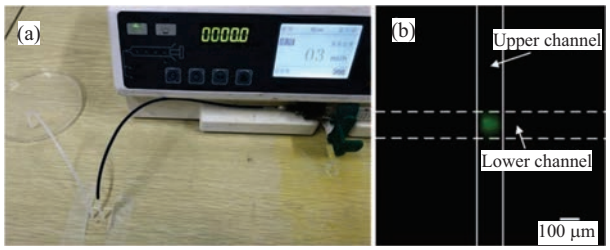

Fig. 7. Test of the fabricated chip: (a) – leakage test under flow rate ranging from 0 to 21 ml/h, and (b) – labeled BSA enrichment under electric field

deformation rate was defined as the area of the channel after bonding to the one before bonding. One could see that higher deformation rate correlated to larger bonding pressure. Under pressure of 0.1 MPa (Fig. 4a), the channel only deformed slightly. After pressure release, the deformation could partially recover. However, at pressure of 0.9 MPa (Fig. 4i), the channel deformed seriously and the final width and depth of the channel significantly decreased, especially for the depth. Fig. 5 shows the influence of bonding pressure on the stress distribution near the micro-channels. The numerical simulation results indicate that the maximum stress lies near the edge of the micro-channel on PDMS interface. This means the channel is apt to break at the interface between two PDMS slabs. The higher maximum stress was associated with larger bonding pressure. Figure 6 indicates the influence of bonding pressure on the deformation rate of the channel. They have a non-linear relationship. Fitted by nonlinear-curve-fit function in OriginPro 8.0 (OriginLab, Massachusetts, USA), an exponential regression was found: $DR = 0.28 - 115.42 \times \exp(-3.58P)$, where DR is deformation rate, and P is the bonding pressure. The coefficient of determination was as high as 99.96%. At bonding pressure of 0.1 MPa, PDMS near the nafion membrane can hardly be bonded. Under pressure larger than 0.3 MPa, however, the channel will significantly deform. Thus in the present work, pressure of 0.2 MPa was applied on PDMS slabs during bonding process.

3.4 Leakage and fluorescence tests

Leakage is one of the most significant problems for microfluidic systems due to the low bonding strength of the chip. Among PMMA, PET, PC, and PDMS chips, the bonding strength of PDMS chips is the lowest, which at an order of magnitude of several hundred kilopascal [28-30]. It is apt to leak during sample injection. Therefore, the fabricated PDMS channel was tested for leakage with red ink, as shown in the Fig. 7(a). The width and depth used for leakage test were 140 μm and 100 μm . Red ink was filled into the channel by injection pump (LSP01-1A, Longer Pump, China). To ensure that the red ink could not be squeezed out from the connection parts, all the connection parts were sealed by the glue. It found there was no leakage until the flow rate increased to 21 ml/h. It indicates that the fabricated PDMS chips can work at a maximum flow rate of 21 ml/h.

Then protein enrichment was performed. The FITC labeled BSA (Bull Serum Albumin), purchased from Beijing bersee science and technology Co.Ltd, was used in the present work. The original concentrate of BSA was 10 mM (mmol/L). It was diluted to 10 M by phosphate buffer saline with PH value of 7.4. Both upper and lower micro-channels were filled by diluted BSA. Four tin wires were used as the electrodes. Two wires were inserted into the reservoirs of the upper micro-channel (upper electrodes), while other two inserted into the reservoirs of the lower one (lower electrodes). The voltage of 20 V was applied on both upper electrodes, voltage of 0 V was applied on lower electrodes. Since nafion membrane has plenty of holes with diameter of 5 nm [31], the overlap of the electric double layer in such small holes leads to the ion selectivity of the chip. The cations are allowed to go through from the holes. The negative charged BSAs flow to the membrane under the electric field and are prevented to go through from the holes. Therefore, the BSAs are enriched near the nafion membrane. Noticeably, the labeled BSA will be concentrated at the anodic side of the membrane. Fig. 7(b) shows the fluorescence image of enriched BSA. The fluorescence intensity increased with time lapse. After 30 s, the fluorescence can be detected by naked eyes under fluorescence microscope (PH100-YG1, Phenix Optics Co., Ltd., China). And at duration of 5 min, its fluorescence intensity nearly reached the highest and only increased slightly after this timeline.

4 Conclusion

In the present work, PDMS chips were fabricated by laser cutting and oxygen plasma bonding for enriching FITC labeled BSA. The numerical simulation models were established for analysis of temperature distribution in PDMS slab during laser cutting and the deformation of the micro-channel during PDMS chip bonding. It was shown that larger width and depth of the micro-channel is associated with higher laser power and lower cutting speed. Higher deformation rate of the bonded micro-channel correlated to larger bonding pressure and followed a simple exponential regression based on bonding pressure. The leakage test demonstrated the fabricated PDMS chip can work at a maximum flow rate of 21 ml/h. The fluorescence test indicated that 10 M BSA can be easily enriched near the nafion membrane under applied voltage.

Acknowledgements

This project is supported by the State Key Laboratory of Alternate Electrical Power System with Renewable Energy Sources (No. LAPS21015) , Open Fund of State Key Laboratory of Luminescent Materials and Devices (No. 2021-skllmd-08) Interdisciplinary Training Program for young teachers and students (No. 415010300081), and Jilin Province Science and Technology Development Plan (No. 20190103067JH). Linlin Sun and Ao Ding contribute equally to the article.

References

[1] G. Xiao, J. He, Y. Qiao, F. Wang, Q. Xia, X. Wang, L. Yu, Z. Lu, and C.-M. Li, "Facile and Low-Cost Fabrication of a Thread/Paper-Based Wearable System for Simultaneous Detection of Lactate and pH in Human Sweat", *Advanced Fiber Materials*, vol. 2, no. 5, pp. 265-278, 2020.

[2] M. Wang, Y. Tan, D. Li, G. Xu, D. Yin, Y. Xiao, T. Xu, X. Chen, X. Zhu, and X. Shi, "Negative Isolation of Circulating Tumor Cells Using a Microfluidic Platform Integrated with Streptavidin-Functionalized PLGA Nanofibers", *Advanced Fiber Materials*, vol. 3, no. 3, pp. 192-202, 2021.

[3] D. Erickson, D. Sinton, and D. Li, "Joule heating and heat transfer in poly (dimethylsiloxane) microfluidic systems", *Lab on a Chip*, vol. 3, no. 3, pp. 141-149, 2003.

[4] C. H. Chen, Y. Lu, M. L. Sin, K. E. Mach, D. D. Zhang, V. Gau, J. C. Liao, and P. K. Wong, "Antimicrobial susceptibility testing using high surface-to-volume ratio microchannels", *Analytical Chemistry*, vol. 82, no. 3, pp. 1012-1019, 2010.

[5] N. A. Papadopoulou, A. B. Florou, and M. I. Prodromidis, "Sensitive determination of iron using disposable Nafion- coated screen-printed graphite electrodes", *Analytical Letters*, vol. 51, no. (1-2), pp. 198-208, 2018.

[6] H. Lee, J. Choi, E. Jeong, S. Baek, H. C. Kim, J.-H. Chae, Y. Koh, S. W. Seo, J.-S. Kim, and S. J. Kim, "dCas9-mediated nanoelectrokinetic direct detection of target gene for liquid biopsy", *Nano letters*, vol. 18, no. 12, pp. 7642-7650, 2018.

[7] A. Perera, D. T. Phan, S. Pudasaini, Y. Liu, and C. Yang, "Enhanced sample pre-concentration by ion concentration polarization on a paraffin coated converging microfluidic paper based analytical platform", *Biomicrofluidics*, vol. 14, no. 1, pp, 014103, 2020.

[8] X. Yang, Z. Yin, L. Li, and H. Zou, "The Fabrication of Poly (methyl methacrylate)(PMMA) Microfluidic Chips by Laser Patterning and Electrohydrodynamic (EHD) Printing", *Lasers in Engineering*, pp, vol 47(1-3), pp. 183-194, 2020.

[9] N. Yang, C. Chen, P. Wang, J. Sun, and H. Mao, "Structure optimization method of microfluidic paper chip based on image grey-level statistics for chromogenic reaction", *Chemical engineering and processing-process Intensification*, vol, 143 pp, , 2019.

[10] R. Chantiwas, S. Park, S. A. Soper, B. C. Kim, S. Takayama, V. Sunkara, H. Hwang, and Y. K. Cho, "Flexible fabrication and applications of polymer nanochannels and nanoslits", *Chemical Society Reviews*, vol. 40, no. 7, pp. 3677-3702, 2011.

[11] Y. C. Chiu, E. M. Brey, and L. V. Perez, "A study of the intrinsic autofluorescence of poly (ethylene glycol)-co-((L)-lactic acid) diacrylate", *Journal of Fluorescence*, vol. 22, no. 3, pp. 907-913, 2012.

[12] Z. Yin and H. Zou, "Experimental and numerical study on PDMS collapse for fabrication of micro/nanochannels", *Journal of Electrical Engineering-Elektrotechnicky Casopis*, vol. 67, no. 6, pp. 414-420, 2016.

[13] S. Schneider, D. Gruner, A. Richter, and P. Loskill, "Membrane integration into PDMS-free microfluidic platforms for organ-on-chip and analytical chemistry applications", *Lab on a Chip*, vol. 21, no. 10, pp. 1866-1885, 2021.

[14] J. B. You, B. Lee, Y. Choi, C.-S. Lee, M. Peter, S. G. Im, and S. S. Lee, "Nanoadhesive layer to prevent protein absorption in a poly(dimethylsiloxane) microfluidic device", *Biotechniques*, vol. 69, no. 1, pp. 47-52, 2020.

[15] Y. Xiangdong, L. Hongzhong, and D. Yucheng, "Research on the cast molding process for high quality PDMS molds", *Microelectronic Engineering*, vol. 86, no. 3, pp. 310-313, 2009.

[16] K. Hyewon, L. Jiyeon, P. Joonhyung, and H. L. Hong, "An improved method of preparing composite poly(dimethylsiloxane) moulds", *Nanotechnology*, vol. 17, no. 1, pp. 197-200, 2006.

[17] T. Wu, C. Ke, and Y. Wang, "Fabrication of trapezoidal cross-sectional microchannels on PMMA with a multi-pass translational method by CO2 laser", *Optik*, vol, 183 pp. 953-961, 2019.

[18] E. Nikolidakis and A. Antoniadis, "FEM modeling simulation of laser engraving", *The International Journal of Advanced Manufacturing Technology*, pp, vol 105(7-8), pp. 3489-3498, 2019.

[19] S. Prakash and S. Kumar, "Experimental investigations and analytical modeling of multi-pass CO2 laser processing on PMMA", *Precision Engineering*, vol, 49 pp. 220-234, 2017.

[20] S. Prakash and S. Kumar, "Fabrication of rectangular cross-sectional microchannels on PMMA with a CO2 laser and underwater fabricated copper mask", *Optics & Laser Technology*, vol, 94 pp. 180-192, 2017.

[21] M. Moradi, O. Mehrabi, T. Azdast, and K. Y. Benyounis, "Enhancement of low power CO2 laser cutting process for injection molded polycarbonate", *Optics & Laser Technology*, vol, 96 pp. 208-218, 2017.

[22] S. Zhang and X. Chen, "CO2 laser ablation of microchannel on PMMA substrate for Koch fractal micromixer", *Journal of the Brazilian Society of Mechanical Sciences and Engineering*, vol. 41, no. 1, pp, 45, 2019.

[23] K. Kheloufi, E. H. Amara, and A. Benzaoui, "Numerical simulation of transient three-dimensional temperature and kerf formation in laser fusion cutting", *Journal of Heat Transfer*, vol. 137, no. 11, pp, 112101, 2015.

[24] P. Nagarajan and D. Yao, "Uniform Shell Patterning Using Rubber-Assisted Hot Embossing Process. II. Process Analysis", *Polymer Engineering and Science*, vol. 51, no. 3, pp. 601-608, 2011.

[25] H. Hocheng and C. C. Nien, "Numerical analysis of effects of mold features and contact friction on cavity filling in the nanoimprinting process", *Journal of Microlithography Microfabrication and Microsystems*, vol. 5, no. 1, pp. 011004, 2006.

[26] Z. Wang, A. A. Volinsky, and N. D. Gallant, "Crosslinking effect on polydimethylsiloxane elastic modulus measured by custom-built compression instrument", *Journal of Applied Polymer Science*, vol. 131, no. 22, pp, , 2014.

[27] K. Myeongsub, M. Byeong-Ui, and C. H. Hidrovo, "Enhancement of the Thermo-mechanical Properties of PDMS Molds for the hot Embossing of PMMA Microfluidic Devices", *Journal of Micromechanics and Microengineering*, vol. 23, no. 9, pp, 095024, 2013.

[28] M. A. Eddings, M. A. Johnson, and B. K. Gale, "Determining the optimal PDMS-PDMS bonding technique for microfluidic devices", *Journal of Micromechanics and Microengineering*, vol. 18, no. 6, pp, , 2008.

[29] V. Sunkara, D. K. Park, and Y. K. Cho, "Versatile method for bonding hard and soft materials", *RSC Advances*, vol. 2, no. 24, pp. 9066-9070, 2012.

[30] K. Kim, S. W. Park, and S. S. Yang, "The optimization of PDMS-PMMA bonding process using silane primer", *Biochip Journal*, vol. 4, no. 2, pp. 148-154, 2010.

[31] W. Ouyang, Z. Li, and J. Han, "Pressure-modulated selective electrokinetic trapping for direct enrichment, purification, and detection of nucleic acids in human serum", *Analytical Chemistry*, vol. 90, no. 19, pp. 11366-11375, 2018.

Received 3 December 2021